

Ab initio molecular orbital studies on the structure, energies, and photodissociation of the electronic excited states of C₂H

Qiang Cui and Keiji Morokuma

Cherry L. Emerson Center for Scientific Computation and Department of Chemistry, Emory University, Atlanta, Georgia 30322

(Received 14 August 1997; accepted 3 October 1997)

High level *ab initio* calculations have been carried out to study seven electronic states of C₂H. The calculated equilibrium structure, energetics and vibrational frequencies for the 3²A' state at the CASPT2/PVTZ level are in good agreement with those obtained experimentally by Hsu *et al.* The transition dipole moments from the ground state C₂H to electronic excited states depend sensitively on the H–C–C bending angle and often peak at nonlinear configurations. Based on this and the dissociation behavior of the excited states, we predict A¹Π_u and c³Σ_u⁺ C₂ fragments to be rich in population, the former of which is experimentally detected recently by Jackson *et al.* The ground X¹Σ_g⁺ and the a³Π_u state C₂ are expected to be formed via the nonadiabatic process 3²A' → 2²A' or 4²A' → 3²A' → 2²A', which is in accord with the experimentally observed lifetime pattern by Hsu *et al.* No reverse barrier for CC–H dissociation was found on the X and A electronic states of C₂H in the linear configuration. The 2²A' state, however, develops a distinct “barrier” (not a true saddle point) along dissociation coordinate when the H–C–C is significantly bent, due to the interaction with upper electronic state. Since the 2²A' state energetically prefers a linear dissociation, we suspect that the upper bound of the CC–H bond energy measured by Hsu *et al.* is not severally affected by this “barrier.” © 1998 American Institute of Physics. [S0021-9606(98)03502-8]

I. INTRODUCTION

The C₂H radical has attracted much attention both experimentally and theoretically over the past several decades due to a number of reasons. Its ground state X²Σ⁺ and the first excited state ²Π are separated by only 3600 cm⁻¹ and undergoes internal conversion upon geometrical changes.¹ The strong and extensive vibronic coupling between the two electronic states hinders the clear characterization of the CCH radical despite extensive spectroscopic studies over the years.² The effects of extensive X–A vibronic interaction along with the Renner–Teller (RT) interaction in the A state complicate the spectra of CCH, and therefore have become the subject of a series of theoretical studies by Peyerimhoff and co-workers.³ The photochemistry of C₂H is also of great interest and has been studied both experimentally⁴ and theoretically⁵ in recent years. Interest in this system also stems from its importance in astrophysics since C₂H is believed to be the major source of C₂ in comets and interstellar media.⁶ Clear understanding of the photodissociation process of C₂H is also needed to characterize accurately the controversial results on the bond energy of CC–H.⁷

In a recent experiment of Hsu *et al.*,⁸ rovibronically (*N, K*–) resolved lifetimes of three vibrational levels of the B state of CCH radical were measured in a supersonic molecular beam. Considerable shorter lifetimes were observed at higher vibrational levels than at level *T* (the assumed B origin), which was interpreted to be predissociation by coupling with X or A levels of CCH via C-type Coriolis interaction. Assuming no barrier exists in the dissociation process of the X and A states, an upper bound of D₀⁰(CC–H) was determined to be 39 388 ± 7 cm⁻¹ (112.62 kcal/mol).

Another interesting quantity that has been investigated by a number of authors is the branching ratio of the photodissociation process. Early studies using photofragment translational spectroscopy produced contradictory results from two experiments^{4(a),9} in Lee's research group. The main difficulty in the assignment of electronic states of C₂ fragments comes from the poor resolution afforded by the time-of-flight (TOF) spectra. In the recent experiments of Jackson *et al.*,¹⁰ spectroscopic resolution is achieved by using laser induced fluorescence (LIF) to analyze the relative population of the photofragments in different electronic states. In this experiment, acetylene was used as the precursor for C₂H and was first photolyzed at 193 nm. The photodissociation products C₂H (X²Σ⁺) and C₂H (A²Π) absorb the photon of the same energy, undergo secondary photodissociation process which at 193 nm can produce the C₂ fragment in the following electronic states: X¹Σ_g⁺, A¹Π_u, B¹Δ_g, B'¹Σ_g⁺, a³Π_u, and b³Σ_g⁻. From simultaneous measurement of the Mulliken (X¹Σ_g⁺–D¹Σ_u⁺) and Freymark (A¹Π_u–E¹Σ_g⁺) systems, and the Deslandres–D'Azumbuja (A¹Π_u–C¹Π_g) and the LeBlanc (B'¹Σ_g⁺–D¹Σ_u⁺) systems, respectively, the nascent population ratio of C₂ in the X:A:B' electronic states was found to be 1:19:1.4. Clearly, nonadiabatic effects have to be involved to produce the ground state C₂ product.

To further understand the experimental results of Hsu *et al.* and that of Jackson *et al.*, theoretical calculations on the dissociation behaviors of the low lying electronic states of C₂H are highly desirable. In the previous theoretical study of Dufflot *et al.*^{5(b)} dissociation curves of C₂H for the lowest 6 electronic states have been calculated at the MRSDCI level. However, the C–C distance was fixed at the equilibrium dis-

tance in the $X^2\Sigma^+$ C₂H during the scan. Since the C–C distance in the excited states is much longer than that in the ground state, the qualitative results might be different and should be examined carefully. In addition, no optimization has been carried out for neither the excited states C₂H nor the crossing structures between different electronic states to characterize the nonadiabatic interactions.

In the current work, we have carried out high level ab initio calculations for the properties of seven electronic states of C₂H. Qualitative dissociation behavior and the nonadiabatic interactions between those electronic states have also been studied. In Sec. II, we summarize the computational methods employed in the current work. In Sec. III, we first discuss the low lying electronic states of the photofragment C₂, followed by the prediction of the properties calculated for several excited states C₂H. Then we discuss the dissociation behavior and the nonadiabatic interactions of those electronic states along the C–H dissociation pathway, and relate these results with the recent experimental findings. In Sec. IV, we make a few conclusions.

II. COMPUTATIONAL METHODS

Geometries of equilibrium structures on the excited state potential surfaces are optimized using the analytical gradient at the complete active space self-consistent field (CASSCF) level, and with a numerical gradient at the CASPT2 (Ref. 11) level with the D95(*d,p*) (Ref. 12) basis set. Several structures have also been optimized with numerical gradient at the CASPT2/PVTZ (Ref. 13) level. The ground and the first excited states have also been optimized with the EOMIP (Ref. 14) PVTZ method, which has been proven to be ideal for radicals with close lying electronic states. The full valence active space, (8*e*/8MO) and (9*e*/9MO), have been used in the CASSCF calculations for both C₂ and C₂H, respectively. In the CASSCF and CASPT2 optimizations for a certain excited state of C₂H, the molecular orbitals are derived from CASSCF (Ref. 15) calculations state-averaged over all the lower states in this irrep (irreducible representation). For example, in the optimization of the $3^2A''$ state, three $2A''$ roots are included in the state-averaged CASSCF calculation. In the CASPT2 calculations, however, the lower states have been projected out using the approximate scheme,¹⁶ and only one root is included. Vibrational frequencies and the zero-point energy (ZPE) are calculated for C₂ and excited state C₂H with the CASPT2 method with double numerical differentiation along with the standard GF matrix scheme, or with numerical differentiation of EOMIP analytical gradient for the ground and the first excited state C₂H with linear structure. Minima on the seam of crossing (MSX) are located also using the analytical gradient at the state-averaged CASSCF level. Detailed discussion for the number of roots included will be given in Sec. III C. Finally single point calculations are performed at the CASPT2/PVTZ level for vertical excitation energies and adiabatic excitation energies. In these single point calculations, the molecular orbitals are consistently obtained from state-averaged CASSCF calculations including 7 roots for the reason which will be discussed in Sec.

III. Furthermore, to investigate the qualitative behavior of the potential energies of these electronic states we consider here, 7-state-averaged CASSCF/D95(*d*) scans have been carried out.

The MOLPRO96 (Ref. 17) was used for all the CASSCF and CASPT2 calculations. Our own program in conjunction with HONDO8.0 has been used for MSX search. EOMIP calculations have been carried out with the ACES-II package.¹⁸

III. RESULTS AND DISCUSSION

A. Electronic states of C₂

To find out how many electronic states we have to include in the calculations consistently and the correlation relationship between C₂H and C₂+H, we first examine the electronic states of the dissociation products C₂. Since the spectroscopic information of C₂ has been well understood experimentally¹⁹ as well as theoretically,²⁰ comparison of our results with those will also give us an idea about the accuracy of the methods we used.

Calculated equilibrium structures, adiabatic excitation energies, and vibrational frequencies along with the corresponding experimental data and some previous calculations are given in Table I for the ten (including degeneracy) lowest electronic states of C₂. As can be seen clearly from Table I, the calculated results with CASPT2/PVTZ agree satisfactorily with all the known experimental parameters.

In Fig. 1, we have shown the potential energy curves of these ten excited states of the C₂ fragment calculated at both the state-averaged CASSCF and CASPT2 level using the 10-state-averaged CASSCF molecular orbital. The results obtained at the two levels are similar qualitatively. It is interesting to note that even though the $c^3\Sigma_u^+$ state is the fourth state (including degeneracy) in adiabatic energy, it is destabilized significantly by the C–C stretch. As C–C is longer than ~ 1.33 Å, it becomes higher in energy than the $A^1\Pi_u$ and $b^3\Sigma_g^-$ states, which both have their equilibrium bond lengths around 1.4 Å. When the C–C distance is stretched up to 1.40 Å, the $c^3\Sigma_u^+$ state becomes even higher than the $B^1\Delta$ and $B'^1\Sigma_g^+$ states and is the highest among those calculated. These results suggest that in principle ten electronic states have to be studied to fully understand the branching ratio from the high-energy experiments of Jackson *et al.*¹⁰ However, we encountered quite a few convergence problems in the preliminary studies, and therefore we wish to truncate the number of electronic states in the current study and leave higher excited states to future work. The most interesting issue in the experiment of Jackson *et al.* is the A:X branching ratio, and therefore one needs to include all the electronic states that can produce the A state dissociation products. According to Fig. 1, we can accomplish this by including at least seven electronic states in the calculation.

B. Equilibrium properties of excited states C₂H

After deciding that seven electronic states of C₂H will be investigated, we have first calculated their equilibrium properties. Optimized geometries, vertical excitation energies,

TABLE I. Properties calculated for the C₂ molecule in several electronic states.^a

State	Method	<i>r</i> _{CC} (Å)	Energetics	Frequency (cm ⁻¹)
<i>X</i> ¹ Σ _g ⁺	CASSCF/I	1.268	-75.627 75	
	CASPT2/I	1.269	-75.721 76	1829
	CASPT2/II	1.253	-75.774 59	1879
	CMRCI+Q ^b	1.246	...	1848
	Expt ^c	1.243	...	1855
<i>a</i> ³ Π _u	CASSCF/I	1.341	0.47	
	CASPT2/I	1.339	0.15	1623
	CASPT2/II	1.323	0.11	1612
	CMRCI+Q ^b	1.316	0.06	1630
	Expt ^c	1.312	0.09	1641
<i>b</i> ³ Σ _g ⁻	CASSCF/I	1.397	1.38	
	CASPT2/I	1.396	1.04	1423
	CASPT2/II	1.379	0.90	1424
	Expt ^c	1.369	0.80	1470
	<i>c</i> ³ Σ _u ⁺	CASSCF/I	1.239	1.23
CASPT2/I		1.240	1.23	1937
CASPT2/II		1.220	1.15	1999
Expt ^c		1.230	1.13	1985
<i>A</i> ¹ Π _u		CASSCF/I	1.349	1.70
	CASPT2/I	1.346	1.26	1567
	CASPT2/II	1.329	1.09	1586
	EOM-CCSD(T) ^d	1.359	1.11	
	Expt ^c	1.318	1.04	1608
<i>B</i> ¹ Δ _g	CASSCF/I	1.419	2.19	
	CASPT2/I	1.415	1.79	1326
	CASPT2/II	1.397	1.63	1362
	EOM-CCSD(T) ^d	1.432	1.56	
	Expt ^c	1.389	1.50	1407
<i>B'</i> ¹ Σ _g ⁺	CASPT2/I	1.409	2.05	1355
	CASPT2/II	1.389	1.96	1374
	EOM-CCSD(T) ^d	1.422	1.92	
	Expt ^c	1.377	1.91	1424

^aTotal energies in hartree have been shown for the *X* ¹Σ_g⁺ in italics. For other electronic states, energies relative to *X* ¹Σ_g⁺ have been shown in eV. Basis I is D95(*d,p*), and basis II is PVTZ.

^bFrom Ref. 20(b).

^cFrom Ref. 19.

^dFrom Ref. 20(a).

adiabatic excitation energies as well as the vibrational frequencies obtained from our calculations are shown in Table II.

The ground *X* ²Σ⁺ and the first excited state *A* ²Π have been well studied by previous theoretical calculations.^{3,5} Good agreement is found for the equilibrium structures as well as for the adiabatic excitation energies between the current work and previous calculations. The C–H dissociation energy from the ground state C₂H has been calculated to be 4.64 eV (107.0 kcal/mol) including ZPE, which is in quite good agreement with the value of 112.4 kcal/mol from the high quality calculation result of Bauschlicher *et al.*⁷ and the value of 112.62 kcal/mol from the latest experimental estimate of Hsu *et al.*⁸

In contrast, there is very limited information about the properties of the excited states of the C₂H. Vertical excitation energies of electronic states within 10 eV have been calculated by a number of authors,^{21,5} and as seen in Table II, the most recent theoretical values are in reasonable agreement with our results. In order to check if diffuse functions are important, we have carried out vertical excitation energy calculations at the CASPT2/III or aug-cc-PVTZ (Ref. 13) level, and the results have been included in Table II. The effect of the diffuse functions is not large, around 0.1 eV. Considering the size of our largest basis set, we feel the *T_v* values of Dufлот *et al.*^{5(b)} for *A* ²Π, 4 ²*A'*, and 2 ²*A''* are underestimated. The characters of the electronic transitions have been analyzed by Dufлот *et al.*,^{5(b)} and none of the excited electronic states in the current study has been found to have significant Rydberg character.

Virtually no information about the equilibrium properties of the excited states of C₂H is known either experimentally or theoretically. It is known that the excited states of C₂H except the *A* ²Π are highly bent,^{5(b)} and have rather flat bending potentials, as can actually be seen from the H–C–C

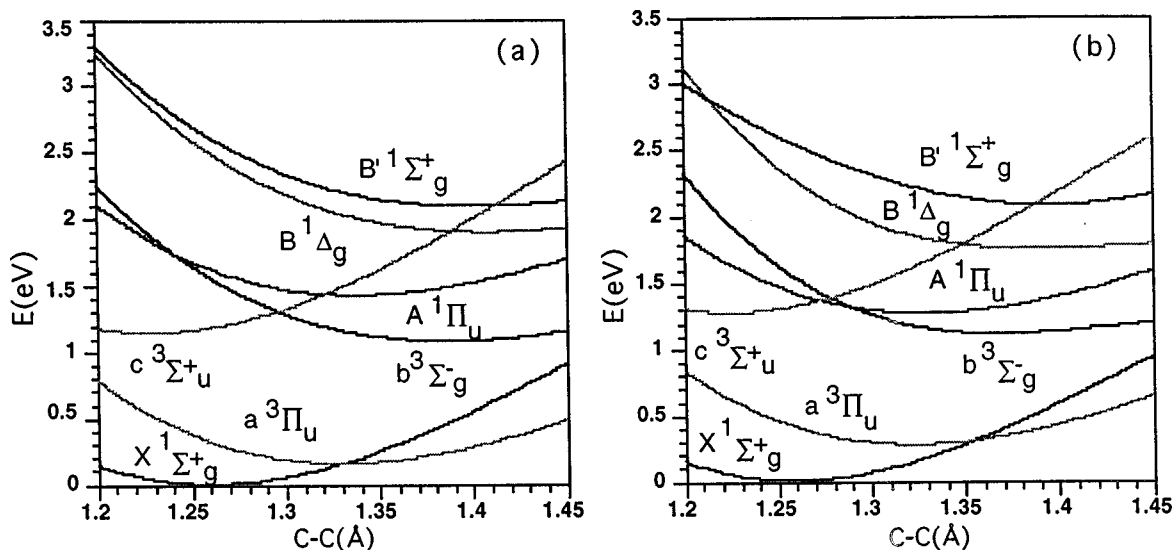


FIG. 1. The potential energies of electronic states of C₂ (in eV) as a function of the C–C distance (Å). (a) Is calculated at the 10-state-averaged CASSCF/PVTZ level, and (b) is calculated at the CASPT2/PVTZ level.

TABLE II. Properties calculated for the C₂H molecule in several electronic states.^a

State	Method ^b	Geometry(Å and deg)			<i>T_v</i> (eV)	<i>T_e</i> (eV)	Frequency (cm ⁻¹)		
		<i>r</i> -CC	<i>r</i> -CH	∠HCC			ω ₃ C-C	ω ₂ bend	ω ₁ C-H
<i>X</i> ² Σ ⁺	CASPT2/II	1.218	1.067	180.00	0.00	<i>-4.64</i>			
	EOMIP/II	1.201	1.056	180.00	0.00		2109	512	3521
	CIPSI ^d	1.223	1.075	180.00	0.00	<i>-4.62</i>	1975	570	3346
	Expt ^e	1.217	1.041	180.00	0.00	<i>-4.88</i>	1848	389	3612
<i>A</i> ² Π	CASPT2/II	1.298	1.074	180.00	0.79	0.50			
	CASPT2/III				0.79				
	EOMIP/II	1.276	1.063	180.00		0.51	1795	571	3424
	CIPSI ^d	1.302	1.064	180.00	0.54	0.44			
<i>3</i> ² <i>A</i> '	Expt ^e	1.288	1.060	180.00		0.45			
	CASSCF/I	1.417	1.144	115.69					
	CASPT2/I	1.411	1.140	113.54			1105	778	2145
	CASPT2/II	1.408	1.130	116.59	6.73	4.86			
	CASPT2/III				6.53				
	CIPSI ^d				6.63				
	MRDCI ^f	1.397	...	113		4.68			
<i>4</i> ² <i>A</i> '	Expt ^g	1.43	...	108.4		4.85 ^g			
	CASSCF/I	1.562	1.148	107.99					
	CASPT2/I	1.546	1.138	110.17			1267	894	2786
	CASPT2/II				7.50	5.80			
<i>2</i> ² <i>A</i> "	CASPT2/III				7.38				
	CIPSI ^d				7.07				
	CASSCF/I	1.533	1.133	119.11					
	CASPT2/I	1.517	1.128	118.56			1017	812	2887
	CASPT2/II				7.50	5.04			
	CASPT2/III				7.38				
<i>3</i> ² <i>A</i> "	CIPSI ^d				7.07				
	MRDCI ^f	1.413	...	115		4.92			
	CASSCF/I	1.547	1.147	105.74					
	CASPT2/I	1.530	1.136	108.12			964	798	2797
	CASPT2/II				7.31	5.51			
MSX (<i>C</i> _{2<i>v</i>})	CIPSI ^d				7.34				
	CASSCF/I	1.267	1.894	70.46					
	CASPT2/II					5.52 ^b			

^aTotal energies of the *X* ²Σ⁺ state with CASPT2/PVTZ is -76.458 384 2 hartree.

^bBasis set I stands for D95(*d,p*), II for cc-PVTZ, and III for aug-cc-PVTZ. For excited states except *A* ²Π, geometry optimizations were done with different state-averaged CASSCF reference wave functions for different states. The vertical and adiabatic excitation energies, however, were obtained with a 7-state-averaged CASSCF reference wave function to ensure balanced treatment. See text for more details.

^cFor *X* ²Σ⁺, the relative energy to the dissociation limit of C₂(²Σ_g⁺) + H(²S) is shown in italic. For other states, adiabatic energies including ZPE corrections are shown.

^dFrom Ref. 5(b).

^eFrom experiments cited in Ref. 5(b).

^fFrom Ref. 5(a).

^gFor Ref. 1. The energy of the "T" level is shown.

^hNo ZPE was included for the MSX structure.

bending curves shown in the Fig. 2(a). Only partially optimized structures of the *3* ²*A*' and *2* ²*A*" states have been presented in the work of Peyerimhoff *et al.*^{5(c)} Experimentally, the origin of the *B* state is also very difficult to measure without ambiguity.¹ Therefore our calculations provide a valuable information in this aspect. As shown in Table II, the predicted equilibrium geometry of the *3* ²*A*' (the *B* state) state is very close to that determined by the experiment of Hsu *et al.*¹ The long C-C distance of more than 1.4 Å reflects the π→π* nature of the state.^{5(b)} The adiabatic energy of 4.86 eV calculated for the *3* ²*A*' state is also rather close to the energy of the "T" vibrational level observed in the

experiment of Hsu *et al.*¹ The calculated harmonic frequencies of 1105 cm⁻¹ for C-C stretch and of 778 cm⁻¹ for the H-C-C bending are fairly close to the energy differences between the three vibrational levels of the *B* state *T*, *T* + 775 cm⁻¹, and *T* + 1221 cm⁻¹ observed by Hsu *et al.*,¹ although they considered 775 cm⁻¹ to correspond to two quanta of bending, 2ν₂. Other excited electronic states, *4* ²*A*', *2* ²*A*", and *3* ²*A*", are relatively high in energy and have a very long equilibrium C-C distance of more than 1.5 Å, reflecting the (π→π*, π→σ) nature of the states.

Transition dipole moments between the lower electronic states are very important quantities in order to understand the

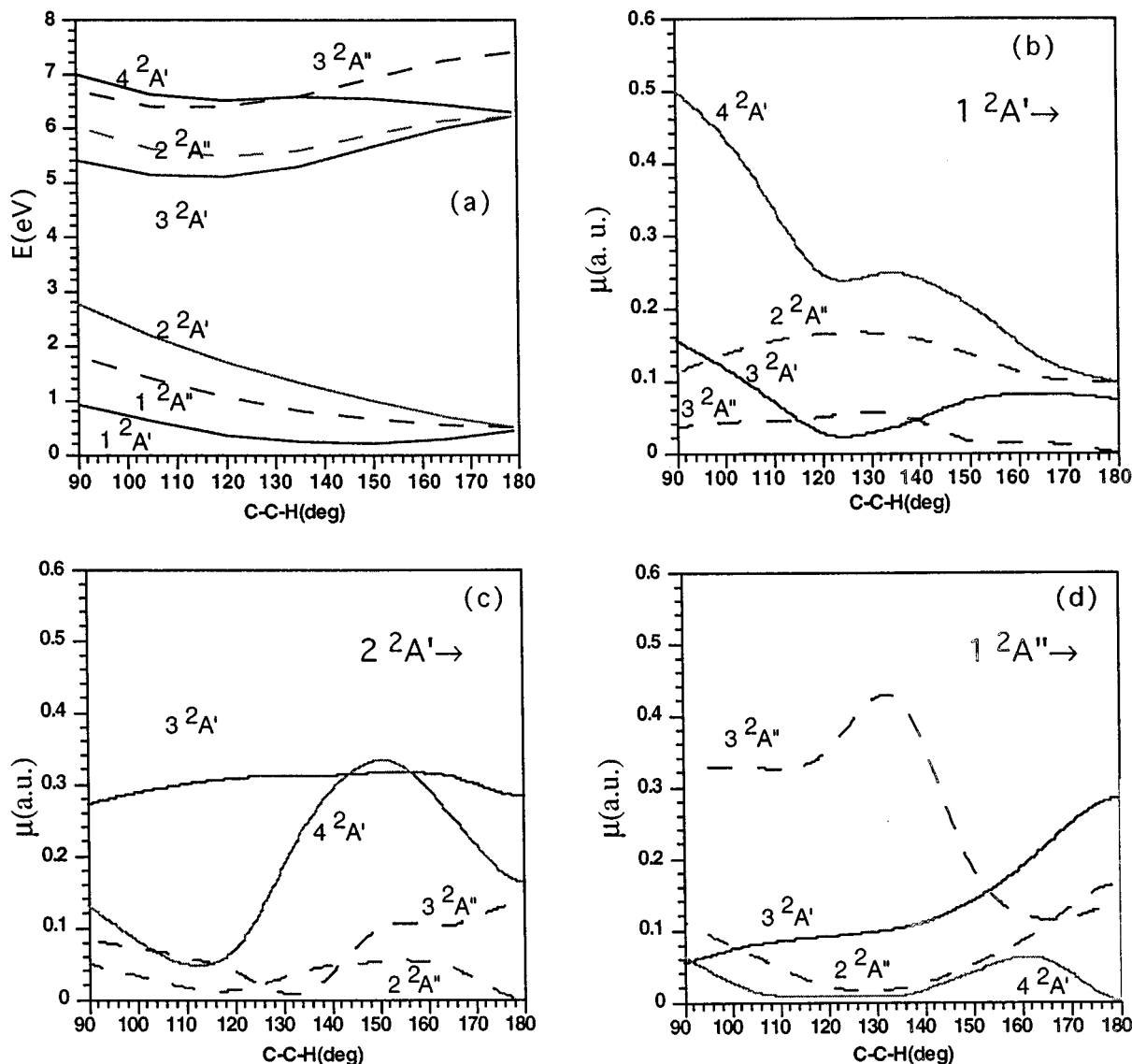


FIG. 2. (a) The bending potential (in eV and deg) calculated at level of 7-state-averaged CASSCF/D95(d,p) for seven electronic states of C_2H with C-C and C-H fixed at 1.35 Å and 1.10 Å, respectively. (b)–(d) transition dipole moments (in a.u.) from the $1^2A'$ ($X^2\Sigma^+$), $2^2A'$ and $1^2A''$ ($A^2\Pi$ pair) states to upper electronic excited states as a function of the H-C-C bending angle (in deg) with C-C and C-H fixed at equilibrium distances of the ground electronic state. Solid lines are for A' states, and dashed lines for A'' states.

branching ratio of the photodissociation products. Since C_2H is produced from the photodissociation of C_2H_2 at 193.3 nm, it is well known that both X and A states of C_2H are produced in their bending excited vibrational states.²² Therefore, the transition dipole moments from the X and A states to upper electronic excited states as functions of the bending angle are required. In the work of Duflet *et al.*,^{5(b)} the transition dipole moments between the ground electronic state to excited states have been calculation only in linear geometry. In Figs. 2(b)–2(d), we have shown the calculated transition dipole moments from the X^2A' , and $2^2A'$, and $1^2A''$ (the latter two corresponding to $A^2\Pi$), respectively, to upper electronic excited states calculated at the level of state-averaged CASSCF/D95(d,p) as functions of the H-C-C bending angle. CASPT2 transition dipole moments have also been calculated at the ground state equilibrium structure and

the state-averaged CASSCF results have been found to be quite reasonable. The basis set of D95(d,p) may not be large enough to yield quantitative transition dipole moments, but it is expected to give qualitatively reliable values for the valence excited states considered here. As seen clearly from Fig. 2, the transition dipole moments depend sensitively on the bending angle and most of them peak at nonlinear geometries. Although it is hard to rationalize these behaviors by a simple orbital picture due to heavy configuration mixture, we can make comments on some bending dependence based on the main configurations of the these electronic states. At linear geometry, the main configurations of the electronic states are $X^2\Sigma^+:(\sigma)^1(\pi)^4$, $A^2\Pi:(\sigma)^2(\pi)^3$, $2^2\Sigma^+(3^2A')$ $(\sigma)^1(\pi)^3(\pi^*)^1$, $2^2\Pi(4^2A'+2^2A''):(\sigma)^2(\pi)^2(\pi^*)^1$ and $2^2\Sigma^-(3^2A''):(\sigma)^1(\pi)^3(\pi^*)^1$, and there are three forbidden transitions, $X^2\Sigma^+ \rightarrow 2^2\Sigma^-(3^2A'')$, $A^2\Pi_{||}(2^2A') \rightarrow$

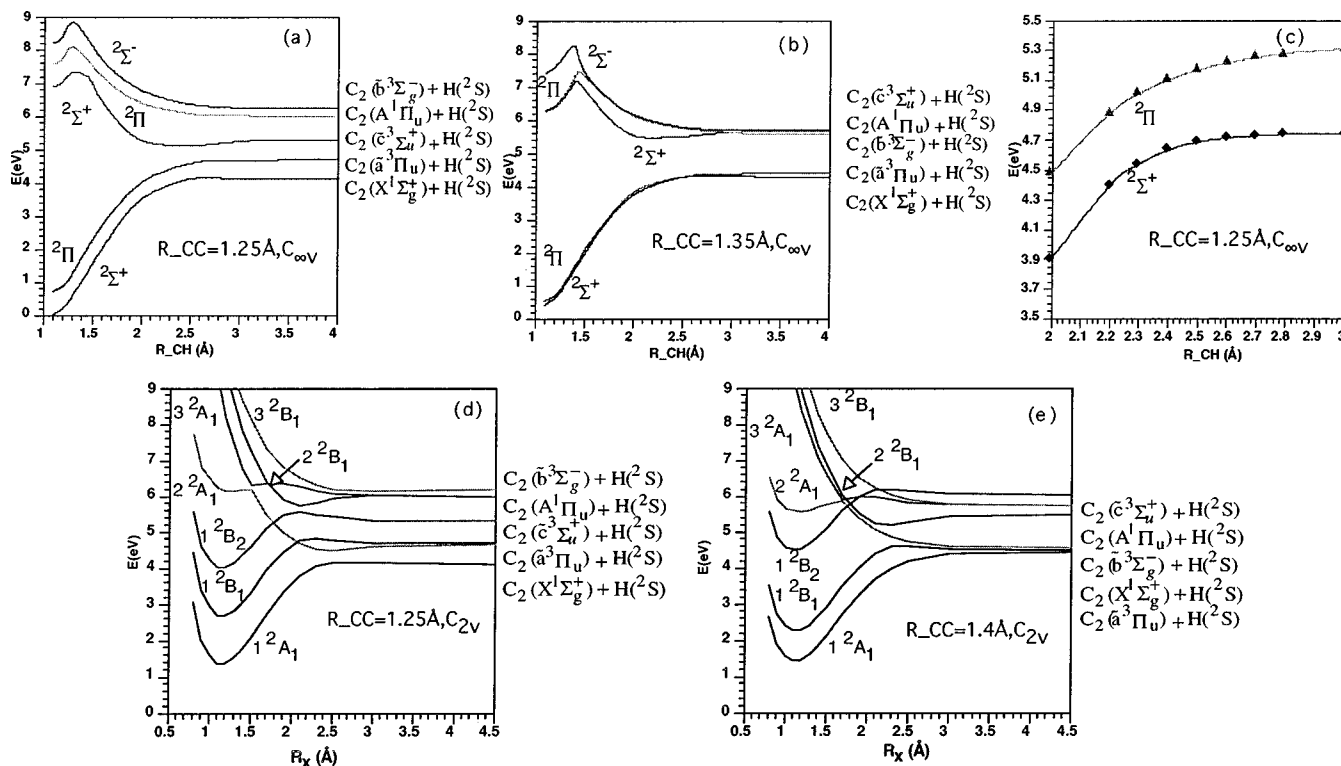


FIG. 3. (a)–(b) Potential energy curves (in eV) calculated at 7-state-averaged CASSCF/D95(*d,p*) level for seven electronic states (including degeneracy) of linear C₂H. The C–C distance is fixed at 1.25 Å and 1.35 Å, in (a) and (b), respectively. (c) Potential energy curves (in eV) calculated at 3-state-averaged CASPT2/D95(*d,p*) level for three electronic states ($X^2\Sigma^+$ and $A^2\Pi$) of linear C₂H. The C–C distance is fixed at 1.25 Å. (d)–(e) Potential energy curves (in eV) calculated at 7-state-averaged CASSCF/D95(*d,p*) level for seven electronic states (including degeneracy) of C₂H in the C_{2v} T-shape arrangement. The abscissa R_x is the distance (in Å) between H and the center of mass of C₂. The C–C distance is fixed at 1.25 Å and 1.40 Å, in (d) and (e), respectively.

$2^2\Pi_{\perp}(2^2A'')$ and $A^2\Pi_{\perp}(2^2A'') \rightarrow 2^2\Pi_{\parallel}(4^2A')$, which are actually confirmed in the results shown in Fig. 2. The main configurations of $X^2\Sigma^+$ and $2^2\Pi$ differ by two spin-orbitals, i.e., the excitation is two electron in nature ($\pi^2 \rightarrow \sigma\pi^*$). As a result, the transition dipole moment between X and $2^2\Pi(4^2A' + 2^2A'')$ is small at linear geometry. As H–C–C bends away from 180.0° and the molecule falls into C_s symmetry, the σ and π_{\parallel} orbitals become heavily mixed. As a result of heavy configuration mixing, the transition dipole moment between X and $2^2\Pi(4^2A' + 2^2A'')$ becomes larger as H–C–C bends away from linearity. The excitation from $A^2\Pi(2^2A' + 2^2A'')$ to the $3^2A'$ state is of $\sigma \rightarrow \pi^*$ type, and the corresponding transition dipole moment is large at linear configuration. The transition dipole moment between the $A' \Pi$ component to $3^2A'$ is hardly changed upon bending because $\sigma \rightarrow \pi_{\parallel}^*$ is not affected very much. On the other hand, the transition dipole moment between the $A'' \Pi$ component to $3^2A'$ decreases dramatically upon bending because $\sigma \rightarrow \pi_{\perp}^*$ is not favored. For the similar reason, the transition dipole moment between the $A' \Pi$ component and $3^2A''$ is smaller in magnitude than that between the $A'' \Pi$ component and $3^2A''$ for nonlinear geometries.

C. Dissociation behavior

In this section, we will discuss the qualitative behavior of the potential energy curves (PECs) of C₂H in these electronic states along the C–H dissociation coordinate. Once

more the energies are calculated with 7-state-averaged full valence CASSCF wave functions, which is expected to give qualitatively correct results. For more quantitative results, one may have to obtain the PECs at higher levels such as MRSDCI. Preliminary results show that CASPT2 is not preferred here due to the poor convergence problem when dealing with many close lying states with same symmetry. Due to the large amount of avoided and allowed crossings between these electronic states, fitting and diabaticization will be a tremendous task and will not be pursued here.

First of all, we examine the dissociation behavior of electronic states involved in the current study in two high symmetry cases; linear $C_{\infty v}$ in Figs. 3(a)–3(c) and T-shape C_{2v} in Figs. 3(d)–3(e). In the linear case the abscissa is simply the C–H distance, while in the later it is the distance R_x from H to the center of mass of C₂.

1. Dissociation in C_{∞v}

The electronic states we have studied in linear geometry are $X^2\Sigma^+$, $A^2\Pi$, $2^2\Sigma^+(B)$, $2^2\Pi$, and $1^2\Sigma^-$ and they dissociate adiabatically to five C₂ + H(²S) states as shown in Figs. 3(a)–3(b). When the C–C distance is short, 1.25 Å in Fig. 3(a), no crossing is found for the electronic states included, because at this C–C distance the energetical order of these C₂H states is the same as that of the corresponding electronic states of the C₂ fragment. The $X^2\Sigma^+$ and the $A^2\Pi$ state both dissociate smoothly without significant bar-

rier. However, a closer look seems to reveal that $X^2\Sigma^+$ and $2^2\Sigma^+$ have some weak interaction at a long C–H distance of ~ 2.5 Å so that $2^2\Sigma^+$ develops a very shallow exit well and $X^2\Sigma^+$ has a nearly negligible exit barrier. The higher excited states $2^2\Sigma^+$, $2^2\Pi$, and $1^2\Sigma^-$ all have some dissociation barriers. As the C–C distance is stretched to 1.35 Å,²³ as shown in Fig. 3(b), all the higher excited states are stabilized to some extent in the Franck–Condon (FC) region. The $X^2\Sigma^+$ and $A^2\Pi$ pair and the $2^2\Sigma^+$ and $2^2\Pi$ pair, respectively, become rather close in energy in the FC region, and the $2^2\Pi$ state becomes nearly degenerate to the $2^2\Sigma^-$ state as the C–H is significantly stretched. The shallow well on the $2^2\Sigma^+$ state becomes more visible at longer C–C distance. It is seen that the higher excited states and the lower states $X^2\Sigma^+$ and $A^2\Pi$ are well separated in linear configurations.

Since the barriers on the $X^2\Sigma^+$ and the $2^2\Pi$ state are of great importance to the accuracy of the C–H bond energy value obtained from the experiment of Hsu *et al.*⁸ (see discussion later), we have carried out more detailed scan for the exit channel of the two (or three including degeneracy) states at the more accurate CASPT2/D95(*d,p*) level with 3-state-averaged CASSCF molecular orbital. As seen from the Fig. 3(c), no barrier exists along C–H dissociation in the linear configuration on either the X or the A electronic state of C₂H.

2. Dissociation in C_{2v}

Next, we looked at another extreme case, C_{2v} dissociation curves where the C₂H is highly bent. In this T-shape arrangement, the electronic states we included are $1-3^2A_1$, $1-3^2B_1$, and 2^2B_2 .²³ Numerous crossings are found in Figs. 3(d)–3(e). The 2^2A_1 state has an avoided crossing with 3^2A_1 around $R_x=1.4$ Å, and also crosses with the 1^2B_2 state and the 1^2B_1 state at $R_x\sim 1.6$ Å and 1.9 Å, respectively. It might look like that 1^2B_2 and 2^2B_1 has an avoided crossing at $R_x=1.9$ Å, but it is actually a strongly avoided crossing between 1^2B_1 and the 2^2B_1 state, as states of different symmetry (B_1/B_2) do not interact. The late barrier on the 1^2B_2 state must come from the interaction with higher B_2 states. As C–C is stretched from 1.25 Å in Fig. 3(d) to 1.4 Å in Fig. 3(e), a few changes are noticed. First of all, since both the order of $2^2\Sigma^+/2^2\Pi$ in C₂H and that of $1^2\Sigma_g^+/3^2\Pi_u$ in C₂ change upon C–C stretch, now the 1^2A_1 C₂H state adiabatically connects to the asymptote of C₂($a^3\Pi_u$) + H(2^2S), while the 2^2A_1 C₂H state connects adiabatically with C₂($X^1\Sigma_g^+$) + H(2^2S). Secondly, since the 1^2B_2 adiabatically connects to the C₂($c^3\Sigma_u^+$) + H(2^2S), which is strongly destabilized upon C–C stretch, the 1^2B_2 state also becomes significantly higher in energy at longer C–C distance. To characterize the nonadiabatic transition from the upper electronic states to the A and X states during the C₂H dissociation, one would like to find the minimum on the seam of crossing (MSX) between these states. In C_{2v} symmetry, the 1^2B_2 and 2^2A_1 MSX is of particular interest since it characterizes the crossing between the B state, which has been probed in the recent experiment of Hsu *et al.*,⁸ and the lower electronic states. We have carried out optimization

of this MSX with a 4-state-averaged CASSCF calculation including only three 2^2A_1 states and one 2^2B_2 state (which makes CPMSCF equations easier to converge). In the single point energy calculations, however, we again used a 7-state-averaged CASSCF to obtain the molecular orbitals to be consistent with other energetics. The obtained MSX structure and energy are presented in Table II. It is seen that the C–C distance is rather short, 1.267 Å, presumably because 1^2B_2 is destabilized at long C–C distance. The energy of the MSX in C_{2v} symmetry at the CASPT2/PVTZ level is 5.52 eV, too high to be accessed in the experiment of the Hsu *et al.*⁸ However, in C_s symmetry, these states (both belonging to $2^2A'$) may undergo avoided crossing at lower energy, through which nonadiabatic transition might take place.

3. Dissociation in C_s

In order to gain insight into the behavior of potential energy surfaces, we carried out CASSCF scans for the C–H dissociation process in C_s symmetry. Selected potential curves along the C–H distance are presented in Fig. 4, and some H–C–C bending potential curves are shown in Fig. 5.

In C_s, the states we included become $1-4^2A'$ and $1-3^2A''$, and larger number of avoided crossings are observed due to extensive interactions between close lying electronic states. While the low lying $1^2A'$ and the $1^2A''$ states dissociate without significant barrier, the $2^2A'$ state is strongly destabilized upon H–C–C bending and develops a distinct dissociation barrier at the C–H distance of about 1.8 Å. This is not to say that there is a saddle point for dissociation on the $2^2\Pi$ state, which has been shown to dissociate without barrier at lower energy in the linear arrangement. The character of this “barrier” on the $2^2A'$ state can be traced back to the diabatic character in C_{2v} symmetry. As can be seen clearly from Fig. 3(d), the electronic state in C_{2v} that correlates to $2^2A'$ in C_s is 1^2B_2 . The 1^2B_2 state correlates to the C₂($c^3\Sigma_u^+$) state in C_{2v}, and therefore crosses with the 2^2A_1 state which correlates to a lower dissociation limit. As one breaks the C_{2v} symmetry to C_s, both the 2^2A_1 and 1^2B_2 fall into the A' symmetry, and the crossing between them becomes a barrier on the lower adiabatic state $2^2A'$. Although the B state $3^2A'$ prefers a long C–C distance in the FC region, it is lower in energy at short C–C distance (~ 1.25 Å) when the C–H is significantly stretched (>1.5 Å). The reason is similar to the case of the 1^2B_2 state in C_{2v}, namely the $3^2A'$ adiabatically connects to the $c^3\Sigma_u^+$ state at short C–C distance, which is destabilized significantly by the C–C stretch, and as a result, the $3^2A'$ state and the lower electronic states are closer in energy only when C–C is short. Indeed, as we have seen in the C_{2v} case, the MSX between the 2^2A_1 ($2^2A'$ in C_s) and the 1^2B_2 ($3^2A'$ in C_s) has a very short C–C distance of 1.267 Å. The $2^2A''$ state is stabilized by C–C stretch at long C–H distances, and becomes very close to the $2^2A'$ state as seen in Fig. 4(d). In C_{2v}, this corresponds to the crossing between 2^2B_1 ($2^2A''$ in C_s) and the 1^2B_2 state ($2^2A'$). The dissociation limit at short C–C distance ~ 1.25 Å is very clear because the electronic states of C₂ are well separated as seen

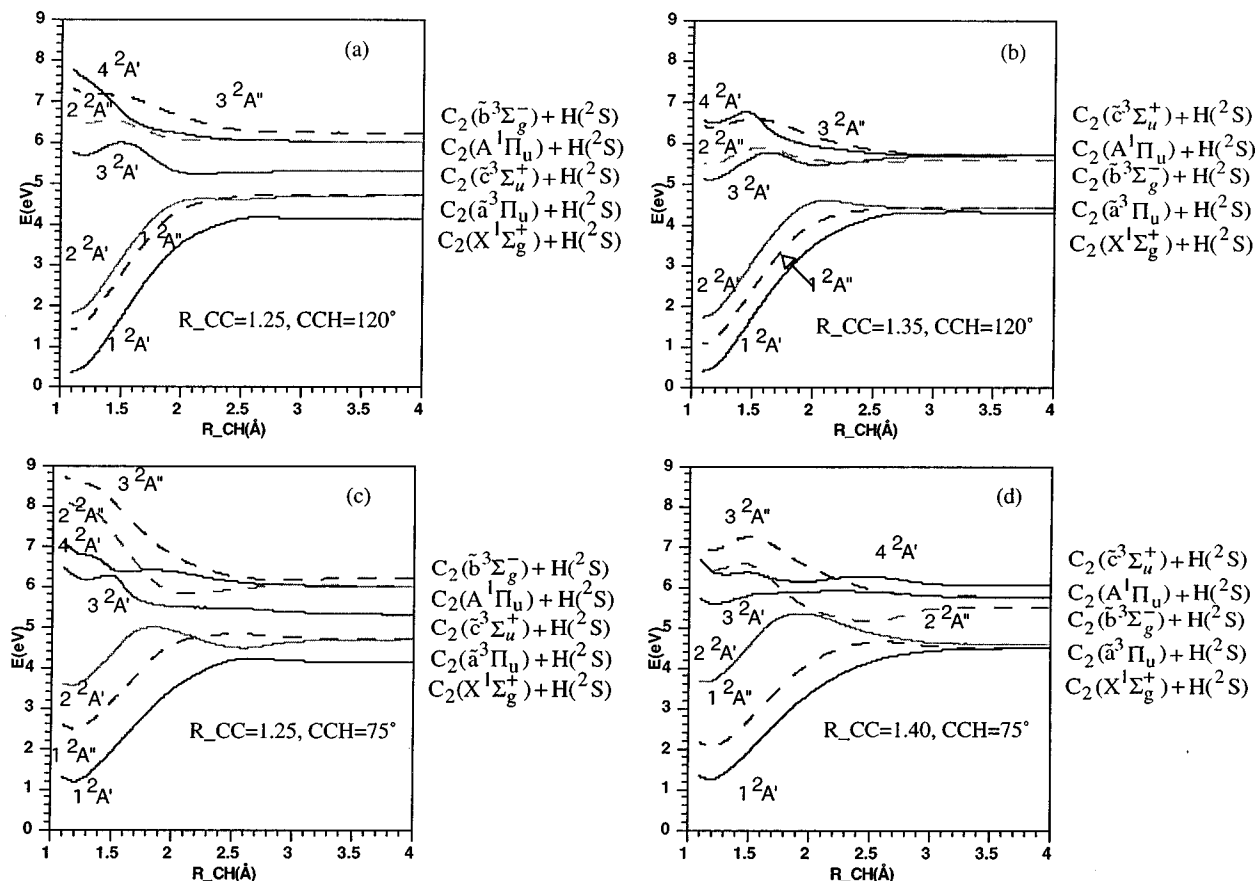


FIG. 4. Potential energy curves (in eV) calculated at 7-state-averaged CASSCF/D95(*d,p*) level for seven electronic states (including degeneracy) of C₂H in C_g symmetry. The C–C distance and H–C–C angles are labeled under each curve. Solid lines are for A' states, and dashed lines for A'' states.

in Fig. 1. At longer C–C distance, however, it is not entirely clear immediately to which state the 4 ²A' correlates, *c* ³Σ_u⁺ or the B ¹Δ_g, due to the crossing between them as illustrated in Fig. 1.

D. Relationship to experiments

In this section, we briefly discuss several aspects of the recent experiments of Jackson *et al.*¹⁰ and Hsu *et al.*,⁸ in conjunction with our calculation results. In the experimental work of Jackson *et al.*,¹⁰ the branching ratio of the C₂ fragment in its X ¹Σ_g⁺, A ¹Π_u, and B' ¹Σ_g⁺ states has been measured to be 1:19:1.4. The population of the other states *b* ³Σ_g⁻, *c* ³Σ_u⁺, and B ¹Δ_g is not clear from their experiment. Taking the value of 1:3 for the X:*a*(³Π_g) ratio from the earlier work of Wodtke and Lee,^{4(a)} the value of 1:3:19:1.4 has been derived for the ratio X:*a*:A':B'. We can try to understand this ratio by reviewing the present results of calculation.

First of all, it is well established from numerous experimental studies^{22,24} that the major product of photodissociation of C₂H₂ at 193.3 nm is C₂H (X ²Σ⁺) with large bending excitation. We recall from Sec. III B and Fig. 2 that the X ²A' state has relatively large transition dipole moment to the 4 ²A' and 2 ²A'' states when H–C–C bending vibration is excited. The excitation energy from X ²A' to 4 ²A' and

2 ²A'' is, as seen in Table II, in the range of 5–7.4 eV, which matches the 193.3 nm photon energy. Therefore, it is most likely that the initial excitation of C₂H at 193.3 nm produces the 4 ²A' and the 2 ²A'' states. As shown in Fig. 4, at short C–C distance of ~1.25 Å where the *c* ³Σ_u⁺ state of C₂ is well below A ¹Π_u and *b* ³Σ_g⁻ states, 4 ²A' and 2 ²A'' of C₂H correlate to A ¹Π_u. This is certainly in accord with the experimental fact that A ¹Π_u has the largest population in the nascent C₂ product.

At longer C–C distance ~1.40 Å which is closer to the equilibrium distance of C₂H in its excited electronic states, Fig. 4 indicates that the 4 ²A' and the 2 ²A'' states of C₂H correlate to the *c* ³Σ_u⁺/B ¹Δ_g and the *b* ³Σ_g⁻ state of C₂, respectively. In addition, as shown in Fig. 4(c), at the short C–C distance, *c* ³Σ_u⁺ can also be formed rather efficiently via the 4 ²A' → 3 ²A' nonadiabatic transition. Therefore, we predict that the *c* ³Σ_u⁺ state should also be rich in population of the C₂ product, which is worth investigating further experimentally.

Nonadiabatic processes can produce a smaller amount of X(¹Σ_g⁺) and *a*(³Π_u) state of the C₂ product. Starting from the 4 ²A' state, two nonadiabatic transitions, 4 ²A' → 3 ²A' → 2 ²A' can produce the 2 ²A' state, which correlates to the X(¹Σ_g⁺) and *a*(³Π_u) state of C₂ at short (1.25 Å) and long (>1.35 Å) C–C distances, respectively. The nonadia-

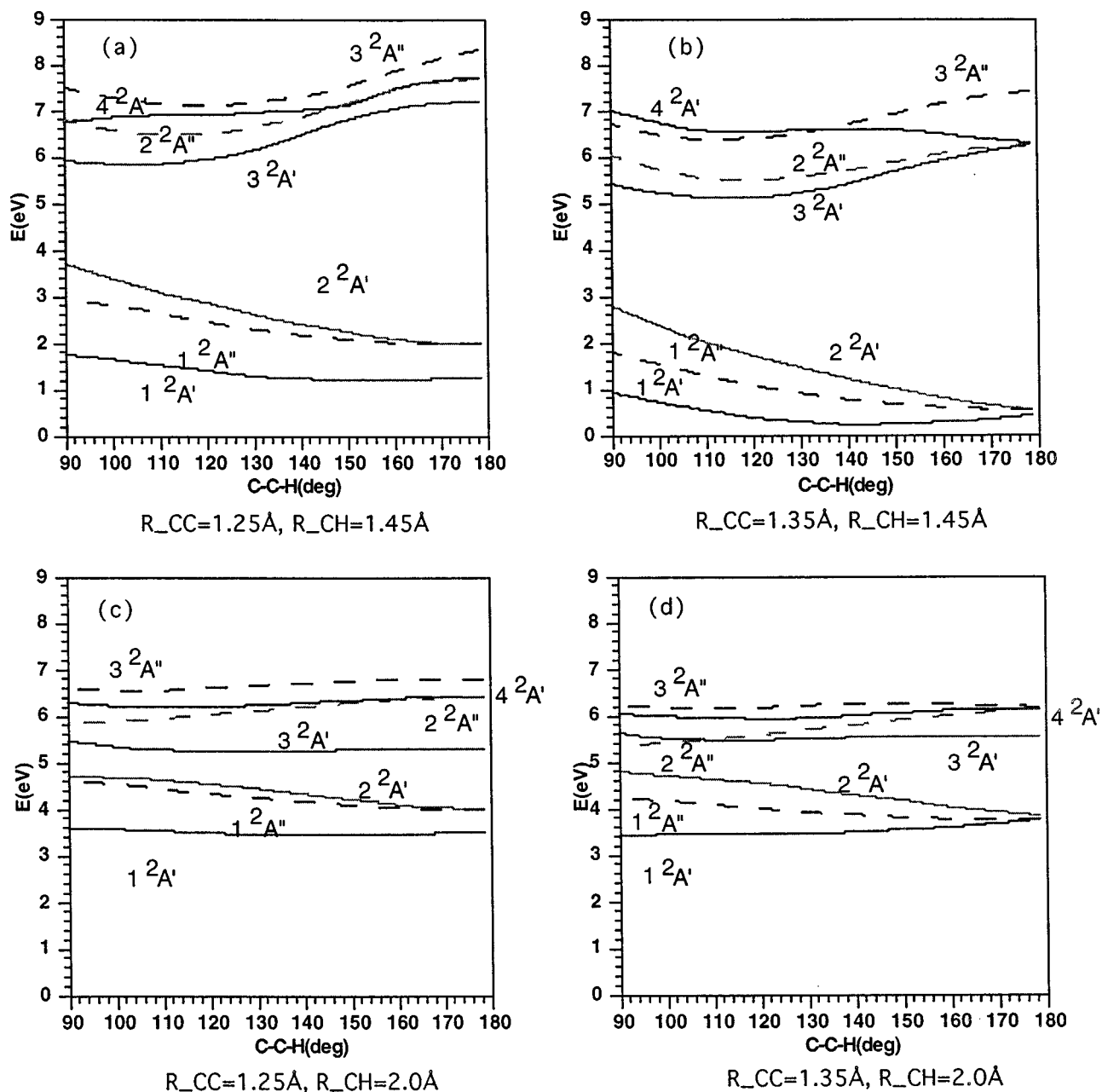


FIG. 5. H-C-C bending potential energy curves (in eV) calculated at 7-state-averaged CASSCF/D95(d,p) level for seven electronic states (including degeneracy) of C_2H in C_g symmetry. The C-C distance and the C-H distance (in Å) are labeled under each curve. Solid lines are for A' states, and dashed lines for A'' states.

batic transition from $2^2A''$ to $2^2A'$ is not expected to be important, since the coupling element has to be Coriolis-type which is usually small in magnitude.

In the recent experiment from Hsu *et al.*⁸ the energetic range studied is much lower. The lifetime of three vibrational levels, T , $T+775$, and $T+1221$, of the B state C_2H have been probed, where the T level is $39\,157.42\text{ cm}^{-1}$ above the ground state zero-point level. Table II indicates that at this energy only the $B\ 3^2A'$ electronic state needs to be considered. According to Figs. 3(d) and 4(c), the quenching of the $3^2A'$ state is possible by making the transition from the $3^2A'$ to the $2^2A'$ state. Indeed, no K^2 dependence in the lifetime has been observed for the rovibrational levels

of the B state experimentally, confirming that the predissociation was not caused by the coupling between A' and A'' states. It was also mentioned that an N^2 dependent lifetime, which is anticipated for C -type Coriolis coupling cases, was not observed at levels T and $T+1221$, although found for the $T+775$ level. Our explanation is that since $2^2A'$ and $3^2A'$ states are coupled via vibrational motion as well as Coriolis coupling, an N^2 dependent lifetime is not guaranteed.

The upper bound of the CC-H dissociation energy has been determined by measuring the rovibronic distributions of C_2 after the photodissociation process.⁸ Therefore, the error in the value depends on how much energy is distributed into the translation of photofragments, which tends to be large if

there is a large reverse barrier. Our calculations [Figs. 3(a) and 3(c)] indicated there is no reverse barrier on the *X* or *A* surface if dissociation takes place in linear configuration. The 2²A' (one of the A²Π pair) develops a distinct "barrier" upon significant (C–C–H) bending. How much will this "barrier" effects the CC–H dissociation energy determined by Hsu *et al.*? We suspect that the effect is not awfully large. Starting from the 3²A' state after excitation, the trajectory will make a nonadiabatic transition to the 2²A' state with a highly bent configuration, producing highly bending excited 2²A'. Figures 5(c) and 5(d) show that the 2²A' state has a strong preference to a linear configuration. Therefore, trajectories will dissociate with most of its energy in bending (which results in product rotation) and very little energy is likely to be released into the translation.

IV. CONCLUSIONS

In the current study, we have carried out *ab initio* calculations to study seven electronic states of C₂H. Equilibrium properties for the excited states have been obtained at a high level of theory CASPT2/PVTZ, and the qualitative dissociation behavior of these electronic states has been investigated with the state-averaged CASSCF method. Based on the results, we have discussed the recent experimental observations of Jackson *et al.*¹⁰ and Hsu *et al.*⁸ The conclusions can be briefly summarized as follows.

- (1) The calculated equilibrium structure, energetics and vibrational frequencies for the 3²A' state are in good agreement with those obtained experimentally by Hsu *et al.*¹ Upon excitation, the equilibrium C–C distance is elongated to ~1.4 Å and the H–C–C angle is highly bent to be ~110°. Other excited states have even longer C–C equilibrium distances, and are higher in energy.
- (2) The transition dipole moments from the ground electronic state and the low lying excited states (A²Π), to higher lying electronic excited states of C₂H depend sensitively on the H–C–C bending angle and often peak at nonlinear configurations. If *X* C₂H is assumed to be the dominant product from the photodissociation of C₂H₂, we expect that the excitation of *X* C₂H at 193.3 nm will produce mainly the 4²A' and 2²A'' states. Based on this and the dissociation behavior of these electronic states, we expect that A¹Π_u and c³Σ_u⁺ C₂ fragment to be rich in population. Indeed, in the experimental work of Jackson *et al.*¹⁰ the *A* state has the largest population among those detected. Although the c³Σ_u⁺ state was not studied in their experiment, it is likely to be formed and is worth being studied in the future.
- (3) The ground X¹Σ_g⁺ and low lying excited state a³Π_u of C₂ are expected to be formed via the nonadiabatic processes from the 4²A' via two nonadiabatic transitions and from the 3²A' state via a nonadiabatic transition to the 2²A' state. The 2²A' state can dissociate directly to the X¹Σ_g⁺ state of C₂ at short C–C distance (~1.25 Å), and to the a³Π_u state of C₂ at long C–C distance (>1.35 Å). This is in accord with the fact that no *K*² dependent lifetime was observed in the experiment of

Hsu *et al.*⁸ which confirms that the predissociation of the *B* state is not via A'–A'' type coupling. Since the 2²A' and 3²A' states can be coupled via vibrational motion in C_s, we argue that the *N*² dependent lifetime is not guaranteed.

- (4) No reverse barrier for CC–H dissociation was found on the *X* and *A* electronic states of C₂H in the linear configuration. The 2²A' state, however, develops a distinct "barrier" (not a true saddle point) along dissociation coordinate when the H–C–C is significantly bent. Since the 2²A' state prefers a linear dissociation energetically, we expect a large amount of bending excitation in C₂H after the 3²A'→2²A' transition, which will produce rotational hot fragment. As a result, we suspect that the upper bound of the CC–H bond energy obtained by Hsu *et al.* is not severally affected by this "barrier."

ACKNOWLEDGMENTS

The authors express their thanks to Professor Y.-C. Hsu and Professor W. M. Jackson for providing us experimental results before publication, and also for many stimulating discussions. The authors also thank Dr. A. Mebel, and Mr. O. Sorkhabi for discussion. Q.C. acknowledges a graduate fellowship from the Phillips Petroleum Co. This work was in part supported by the Grant F49620-95-1-0182 from the Air Force Office of Scientific Research.

¹ See, for example, Y.-C. Hsu, Y.-J. Shiu, and C.-M. Lin, *J. Chem. Phys.* **103**, 5919 (1995).

² See, for example, Refs. 1–26 in Ref. 1.

³ (a) M. Peric, W. Reuter, and S. D. Peyerimhoff, *J. Mol. Spectrosc.* **148**, 201 (1991); (b) H. Thümmel, M. Peric, S. D. Peyerimhoff, and R. J. Buenker, *Z. Phys. D* **13**, 307 (1989); (c) M. Peric, R. J. Buenker, and S. D. Peyerimhoff, *Mol. Phys.* **71**, 673 (1990); (d) M. Peric, S. D. Peyerimhoff, and R. J. Buenker, *ibid.* **71**, 693 (1990); (e) *J. Mol. Spectrosc.* **148**, 180 (1991); (f) *Z. Phys. D* **24**, 177 (1992).

⁴ (a) A. M. Wodtke and Y. T. Lee, *J. Phys. Chem.* **89**, 4744 (1985); (b) V. M. Blunt, H. Lin, O. Sorkhabi, and W. M. Jackson, *Chem. Phys. Lett.* **257**, 347 (1996), and references therein; (c) P. M. Goodwon and T. A. Cool, *J. Chem. Phys.* **89**, 6600 (1988).

⁵ (a) S.-K. Shih, S. D. Peyerimhoff, and R. J. Buenker, *J. Mol. Spectrosc.* **74**, 124 (1979); (b) D. Duflo, J.-M. Robbe, and J.-P. Flament, *J. Chem. Phys.* **100**, 1236 (1994).

⁶ W. M. Jackson, V. M. Blunt, H. Lin, M. Green, G. Olivera, W. H. Fink, Y. Bao, R. S. Urdahl, F. Mohammad, and M. Zahedi, *Astrophys. Space Sci.* **236**, 29 (1996).

⁷ See, for example, H. Partridge and C. W. Bauschlicher, Jr., *J. Chem. Phys.* **103**, 10589 (1995).

⁸ W.-C. Chiang, and Y.-C. Hsu (private communication).

⁹ B. A. Balko, J. Zhang, and Y. T. Lee, *J. Chem. Phys.* **94**, 7958 (1991).

¹⁰ O. Sorkhabi, V. M. Blunt, H. Lin, D. Xu, J. Wrobel, R. Price, and W. M. Jackson, *J. Chem. Phys.* (submitted).

¹¹ See, for example, K. Anderson, B. Roos, in *Modern Electronic Structure Theory*, edited by D. Yarkony (World Scientific, Singapore, 1995).

¹² T. H. Dunning, Jr., *J. Chem. Phys.* **53**, 2823 (1970).

¹³ T. H. Dunning, Jr., *J. Chem. Phys.* **90**, 1007 (1989).

¹⁴ See, for example, J. F. Stanton and J. Gauss, *J. Chem. Phys.* **101**, 8938 (1994).

¹⁵ See, for example, H.-J. Werner, *Adv. Chem. Phys.* **LXIX**, 1 (1987).

¹⁶ P. J. Knowles and H.-J. Werner, *Theor. Chim. Acta* **84**, 95 (1992).

¹⁷ MOLPRO96.4, P. J. Knowles and H.-J. Werner, University of Birmingham, 1996.

¹⁸ ACES II, J. F. Stanton, J. Gauss, W. J. Lauderdale, J. D. Watts, and R. J. Bartlett, Quantum Theory Project, University of Florida, 1994.

¹⁹ (a) K. P. Huber and G. Herzberg, *Molecular Spectra and Molecular Struc-*

ture IV. *Constants of Diatomic Molecules* (Van Nostrand, Princeton, 1979); (b) M. Martin, *J. Photochem. Photobiol. A* **66**, 263 (1992).

²⁰See, for example (a) J. D. Watts and R. J. Bartlett, *Chem. Phys. Lett.* **233**, 81 (1995); (b) K. A. Peterson, *J. Chem. Phys.* **102**, 626 (1995).

²¹A. G. Koures and L. B. Harding, *J. Phys. Chem.* **95**, 1035 (1991).

²²See, for example, Y.-C. Hsu, F.-T. Chen, L.-C. Chou, and Y.-J. Shiu, *J. Chem. Phys.* **105**, 9153 (1996).

²³Although we noticed in a previous section that the $c^3\Sigma_u^+$ state becomes

higher in energy than the $B^1\Delta_g$ and $B'^1\Sigma_g^+$ states when C-C is stretched beyond 1.35 Å, the same seven asymptotic states as in the linear case have been obtained due to symmetry reason. The $B^1\Delta_g$ and $B'^1\Sigma_g^+$ states + H(²S) which correspond to $4^2A_1/4^2B_1$ and 5^2A_1 , respectively, in C₂H are not included.

²⁴Y.-C. Hsu, F.-T. Chen, L.-C. Chou, and Y.-J. Shiu, *J. Chem. Phys.* **98**, 6690 (1993).